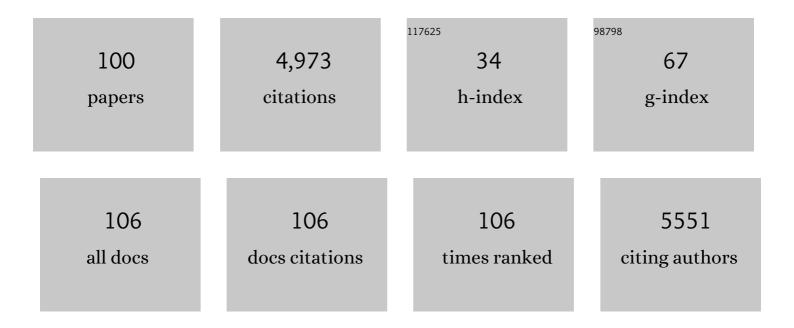
Mark D Pagel

List of Publications by Year in descending order

Source: https://exaly.com/author-pdf/6276057/publications.pdf Version: 2024-02-01



MARK D PACEL

#	Article	IF	CITATIONS
1	Radiometal-Based PET/MRI Contrast Agents for Sensing Tumor Extracellular pH. Biosensors, 2022, 12, 134.	4.7	5
2	Review and consensus recommendations on clinical <scp>APT</scp> â€weighted imaging approaches at <scp>3T</scp> : Application to brain tumors. Magnetic Resonance in Medicine, 2022, 88, 546-574.	3.0	79
3	Quantitative Apparent Diffusion Coefficients From Peritumoral Regions as Early Predictors of Response to Neoadjuvant Systemic Therapy in <scp>Tripleâ€Negative</scp> Breast Cancer. Journal of Magnetic Resonance Imaging, 2022, 56, 1901-1909.	3.4	6
4	Tumor necrosis by pretreatment breast MRI: association with neoadjuvant systemic therapy (NAST) response in triple-negative breast cancer (TNBC). Breast Cancer Research and Treatment, 2021, 185, 1-12.	2.5	10
5	Abstract PD6-07: Volumetric changes on longitudinal dynamic contrast enhanced MR imaging (DCE-MRI) as an early treatment response predictor to neoadjuvant systemic therapy (NAST) in triple negative breast cancer (TNBC) patients. , 2021, , .		0
6	Abstract PD6-06: Radiomic phenotypes from dynamic contrast-enhanced MRI (DCE-MRI) parametric maps for early prediction of response to neoadjuvant systemic therapy (NAST) in triple negative breast cancer (TNBC) patients. , 2021, , .		1
7	Functional Tumor Volume by Fast Dynamic <scp>Contrastâ€Enhanced MRI</scp> for Predicting Neoadjuvant Systemic Therapy Response in <scp>Tripleâ€Negative</scp> Breast Cancer. Journal of Magnetic Resonance Imaging, 2021, 54, 251-260.	3.4	18
8	AcidoCEST MRI Evaluates the Bone Microenvironment in Multiple Myeloma. Molecular Imaging and Biology, 2021, 23, 865-873.	2.6	6
9	Assessment of Early Response to Neoadjuvant Systemic Therapy in Triple-Negative Breast Cancer Using Amide Proton Transfer–weighted Chemical Exchange Saturation Transfer MRI: A Pilot Study. Radiology Imaging Cancer, 2021, 3, e200155.	1.6	12
10	Computer-aided detection of mantle cell lymphoma on F-FDG PET/CT using a deep learning convolutional neural network. American Journal of Nuclear Medicine and Molecular Imaging, 2021, 11, 260-270.	1.0	2
11	Development of a Nanoscale Chemical Exchange Saturation Transfer Magnetic Resonance Imaging Contrast Agent That Measures pH. ACS Nano, 2021, 15, 20678-20688.	14.6	4
12	Simultaneous Evaluations of pH and Enzyme Activity with a CEST MRI Contrast Agent. ACS Sensors, 2021, 6, 4535-4544.	7.8	2
13	Measuring Kidney Perfusion, pH, and Renal Clearance Consecutively Using MRI and Multispectral Optoacoustic Tomography. Molecular Imaging and Biology, 2020, 22, 494-503.	2.6	13
14	Machine Segmentation of Pelvic Anatomy in MRI-Assisted Radiosurgery (MARS) for Prostate Cancer Brachytherapy. International Journal of Radiation Oncology Biology Physics, 2020, 108, 1292-1303.	0.8	18
15	MetNet: Computer-aided segmentation of brain metastases in post-contrast T1-weighted magnetic resonance imaging. Radiotherapy and Oncology, 2020, 153, 189-196.	0.6	32
16	Computer-aided Detection of Brain Metastases in T1-weighted MRI for Stereotactic Radiosurgery Using Deep Learning Single-Shot Detectors. Radiology, 2020, 295, 407-415.	7.3	74
17	Assessments of tumor metabolism with CEST MRI. NMR in Biomedicine, 2019, 32, e3943.	2.8	62
18	Deep learning application engine (DLAE): Development and integration of deep learning algorithms in medical imaging. SoftwareX, 2019, 10, 100347.	2.6	5

Mark D Pagel

#	Article	IF	CITATIONS
19	Extracellular acidosis differentiates pancreatitis and pancreatic cancer in mouse models using acidoCEST MRI. Neoplasia, 2019, 21, 1085-1090.	5.3	18
20	Differentiating lung cancer and infection based on measurements of extracellular pH with acidoCEST MRI. Scientific Reports, 2019, 9, 13002.	3.3	20
21	Dominant words rise to the top by positive frequency-dependent selection. Proceedings of the National Academy of Sciences of the United States of America, 2019, 116, 7397-7402.	7.1	11
22	Recommendations for Reviewers of Biomedical Imaging Grant Applications. Molecular Imaging and Biology, 2019, 21, 612-619.	2.6	0
23	Calcium carbonate nanoparticles stimulate tumor metabolic reprogramming and modulate tumor metastasis. Nanomedicine, 2019, 14, 169-182.	3.3	25
24	Machine learning improves classification of preclinical models of pancreatic cancer with chemical exchange saturation transfer MRI. Magnetic Resonance in Medicine, 2019, 81, 594-601.	3.0	6
25	Differentiation of Myositis-Induced Models of Bacterial Infection and Inflammation with T2-Weighted, CEST, and DCE-MRI. Tomography, 2019, 5, 283-291.	1.8	7
26	Preliminary Results that Assess Metformin Treatment in a Preclinical Model of Pancreatic Cancer Using Simultaneous [18F]FDG PET and acidoCEST MRI. Molecular Imaging and Biology, 2018, 20, 575-583.	2.6	29
27	Characterization of Dâ€maltose as a T ₂ â€exchange contrast agent for dynamic contrastâ€enhanced MRI. Magnetic Resonance in Medicine, 2018, 80, 1158-1164.	3.0	10
28	The deep history of the number words. Philosophical Transactions of the Royal Society B: Biological Sciences, 2018, 373, 20160517.	4.0	23
29	Detection of Enzyme Activity and Inhibition during Studies in Solution, In Vitro and In Vivo with CatalyCEST MRI. Molecular Imaging and Biology, 2018, 20, 240-248.	2.6	23
30	A comparison of exogenous and endogenous <scp>CEST</scp> <scp>MRI</scp> methods for evaluating in vivo p <scp>H</scp> . Magnetic Resonance in Medicine, 2018, 79, 2766-2772.	3.0	49
31	Linearization improves the repeatability of quantitative dynamic contrast-enhanced MRI. Magnetic Resonance Imaging, 2018, 47, 16-24.	1.8	11
32	Clinical applications of chemical exchange saturation transfer (CEST) MRI. Journal of Magnetic Resonance Imaging, 2018, 47, 11-27.	3.4	203
33	A light-fluence-independent method for the quantitative analysis of dynamic contrast-enhanced multispectral optoacoustic tomography (DCE MSOT). Photoacoustics, 2018, 10, 54-64.	7.8	21
34	Parallel Accumulation of Tumor Hyaluronan, Collagen, and Other Drivers of Tumor Progression. Clinical Cancer Research, 2018, 24, 4798-4807.	7.0	65
35	A Comparison of Iron Oxide Particles and Silica Particles for Tracking Organ Recellularization. Molecular Imaging, 2018, 17, 153601211878732.	1.4	3
36	Noninvasive detection of enzyme activity in tumor models of human ovarian cancer using catalyCEST MRI. Magnetic Resonance in Medicine, 2017, 77, 2005-2014.	3.0	34

MARK D PAGEL

#	Article	IF	CITATIONS
37	A biomarker-responsive T _{2ex} MRI contrast agent. Magnetic Resonance in Medicine, 2017, 77, 1665-1670.	3.0	11
38	Detection of DTâ€diaphorase Enzyme with a ParaCEST MRI Contrast Agent. Chemistry - A European Journal, 2017, 23, 6514-6517.	3.3	14
39	Clinical Translation of Tumor Acidosis Measurements with AcidoCEST MRI. Molecular Imaging and Biology, 2017, 19, 617-625.	2.6	74
40	Managers of Molecular Imaging Laboratories (MOMIL) Interest Group. Molecular Imaging and Biology, 2017, 19, 332-335.	2.6	0
41	Multislice CEST MRI improves the spatial assessment of tumor pH. Magnetic Resonance in Medicine, 2017, 78, 97-106.	3.0	27
42	Detecting <i>in vivo</i> urokinase plasminogen activator activity with a catalyCEST MRI contrast agent. NMR in Biomedicine, 2017, 30, e3721.	2.8	14
43	Q&A: What is human language, when did it evolve and why should we care?. BMC Biology, 2017, 15, 64.	3.8	19
44	Chapter 13 Responsive paraCEST MRI Contrast Agents and Their Biomedical Applications. , 2017, , 283-310.		0
45	Imaging Lung Cancer by Using Chemical Exchange Saturation Transfer MRI With Retrospective Respiration Gating. Tomography, 2017, 3, 201-210.	1.8	6
46	Recent Advances in Targeting Tumor Energy Metabolism with Tumor Acidosis as a Biomarker of Drug Efficacy. Journal of Cancer Science & Therapy, 2016, 08, 20-29.	1.7	18
47	A CatalyCEST MRI Contrast Agent that Can Simultaneously Detect Two Enzyme Activities. ChemBioChem, 2016, 17, 383-387.	2.6	17
48	Detection of Sulfatase Enzyme Activity with a CatalyCEST MRI Contrast Agent. Chemistry - A European Journal, 2016, 22, 6491-6495.	3.3	16
49	Advances in Magnetic Resonance Imaging Contrast Agents for Biomarker Detection. Annual Review of Analytical Chemistry, 2016, 9, 95-115.	5.4	57
50	Diamagnetic Imaging Agents with a Modular Chemical Design for Quantitative Detection of β-Galactosidase and β-Glucuronidase Activities with CatalyCEST MRI. Bioconjugate Chemistry, 2016, 27, 2549-2557.	3.6	20
51	QUESPOWR MRI: QUantification of Exchange as a function of Saturation Power On the Water Resonance. Journal of Magnetic Resonance, 2016, 270, 56-70.	2.1	5
52	Detection of Alkaline Phosphatase Enzyme Activity with a CatalyCEST MRI Biosensor. ACS Sensors, 2016, 1, 857-861.	7.8	30
53	Respiration gating and Bloch fitting improve pH measurements with acidoCEST MRI in an ovarian orthotopic tumor model. Proceedings of SPIE, 2016, 9788, .	0.8	13
54	Assessing Metabolic Changes in Response to mTOR Inhibition in a Mantle Cell Lymphoma Xenograft Model Using AcidoCEST MRI. Molecular Imaging, 2016, 15, 153601211664543.	1.4	18

MARK D PAGEL

#	Article	IF	CITATIONS
55	A single diamagnetic catalyCEST MRI contrast agent that detects cathepsin B enzyme activity by using a ratio of two CEST signals. Contrast Media and Molecular Imaging, 2016, 11, 130-138.	0.8	32
56	Design and optimization of pulsed Chemical Exchange Saturation Transfer MRI using a multiobjective genetic algorithm. Journal of Magnetic Resonance, 2016, 263, 184-192.	2.1	9
57	A comparison of iopromide and iopamidol, two acidoCEST MRI contrast media that measure tumor extracellular pH. Contrast Media and Molecular Imaging, 2015, 10, 446-455.	0.8	72
58	Double agents and secret agents: the emerging fields of exogenous chemical exchange saturation transfer and T2-exchange magnetic resonance imaging contrast agents for molecular imaging. Research and Reports in Nuclear Medicine, 2015, 5, 19.	1.0	13
59	Evaluating pH in the Extracellular Tumor Microenvironment Using CEST MRI and Other Imaging Methods. Advances in Radiology, 2015, 2015, 1-25.	0.7	102
60	A review of responsive MRI contrast agents: 2005–2014. Contrast Media and Molecular Imaging, 2015, 10, 245-265.	0.8	168
61	Measuring Extracellular pH in a Lung Fibrosis Model with acidoCEST MRI. Molecular Imaging and Biology, 2015, 17, 177-184.	2.6	36
62	Evaluations of Tumor Acidosis Within In Vivo Tumor Models Using Parametric Maps Generated with AcidoCEST MRI. Molecular Imaging and Biology, 2015, 17, 488-496.	2.6	63
63	Bantu expansion shows that habitat alters the route and pace of human dispersals. Proceedings of the National Academy of Sciences of the United States of America, 2015, 112, 13296-13301.	7.1	223
64	Assessment of carbonic anhydrase IX expression and extracellular pH in B-cell lymphoma cell line models. Leukemia and Lymphoma, 2015, 56, 1432-1439.	1.3	36
65	Diffusion MRI with Semi-Automated Segmentation Can Serve as a Restricted Predictive Biomarker of the Therapeutic Response of Liver Metastasis. Magnetic Resonance Imaging, 2015, 33, 1267-1273.	1.8	11
66	Reproducibility of Magnetic Resonance Perfusion Imaging. PLoS ONE, 2014, 9, e89797.	2.5	15
67	Evaluations of extracellular pH within in vivo tumors using acidoCEST MRI. Magnetic Resonance in Medicine, 2014, 72, 1408-1417.	3.0	168
68	The reciprocal linear QUEST analysis method facilitates the measurements of chemical exchange rates with CEST MRI. Contrast Media and Molecular Imaging, 2014, 9, 252-258.	0.8	21
69	The Hanesâ€Woolf linear QUESP method improves the measurements of fast chemical exchange rates with CEST MRI. Magnetic Resonance in Medicine, 2014, 71, 1603-1612.	3.0	50
70	Detecting Enzyme Activities with Exogenous MRI Contrast Agents. Chemistry - A European Journal, 2014, 20, 9840-9850.	3.3	34
71	Comparison of analytical and numerical analysis of the reference region model for DCE-MRI. Magnetic Resonance Imaging, 2014, 32, 845-853.	1.8	2
72	Detection of in vivo enzyme activity with CatalyCEST MRI. Magnetic Resonance in Medicine, 2014, 71, 1221-1230.	3.0	49

Mark D Pagel

#	Article	IF	CITATIONS
73	A CatalyCEST MRI Contrast Agent That Detects the Enzyme-Catalyzed Creation of a Covalent Bond. Journal of the American Chemical Society, 2013, 135, 6396-6398.	13.7	61
74	A reference agent model for DCE MRI can be used to quantify the relative vascular permeability of two MRI contrast agents. Magnetic Resonance Imaging, 2013, 31, 900-910.	1.8	7
75	A linear algorithm of the reference region model for DCE-MRI is robust and relaxes requirements for temporal resolution. Magnetic Resonance Imaging, 2013, 31, 497-507.	1.8	33
76	CEST and PARACEST MRI Contrast Agents for Imaging Cancer Biomarkers. , 2012, , 689-713.		0
77	Imaging in Vivo Extracellular pH with a Single Paramagnetic Chemical Exchange Saturation Transfer Magnetic Resonance Imaging Contrast Agent. Molecular Imaging, 2012, 11, 7290.2011.00026.	1.4	64
78	A nano-sized PARACEST-fluorescence imaging contrast agent facilitates and validates <i>in vivo</i> CEST MRI detection of glioma. Nanomedicine, 2012, 7, 1827-1837.	3.3	34
79	Imaging biomarkers to monitor response to the hypoxia-activated prodrug TH-302 in the MiaPaCa2 flank xenograft model. Magnetic Resonance Imaging, 2012, 30, 1002-1009.	1.8	23
80	Measuring in vivo tumor pHe with CESTâ€FISP MRI. Magnetic Resonance in Medicine, 2012, 67, 760-768.	3.0	100
81	Improved pH measurements with a single PARACEST MRI contrast agent. Contrast Media and Molecular Imaging, 2012, 7, 26-34.	0.8	59
82	Imaging in vivo extracellular pH with a single paramagnetic chemical exchange saturation transfer magnetic resonance imaging contrast agent. Molecular Imaging, 2012, 11, 47-57.	1.4	63
83	A selfâ€calibrating PARACEST MRI contrast agent that detects esterase enzyme activity. Contrast Media and Molecular Imaging, 2011, 6, 219-228.	0.8	54
84	Fluorescent and Lanthanide Labeling for Ligand Screens, Assays, and Imaging. Methods in Molecular Biology, 2011, 716, 89-126.	0.9	21
85	Responsive paramagnetic chemical exchange saturation transfer MRI contrast agents. Imaging in Medicine, 2011, 3, 377-380.	0.0	0
86	The hope and hype of multimodality imaging contrast agents. Nanomedicine, 2011, 6, 945-948.	3.3	18
87	PARACEST MRI with improved temporal resolution. Magnetic Resonance in Medicine, 2009, 61, 399-408.	3.0	74
88	An amine-derivatized, DOTA-loaded polymeric support for Fmoc solid phase peptide synthesis. Tetrahedron Letters, 2009, 50, 4459-4462.	1.4	31
89	Tracking the Relative In Vivo Pharmacokinetics of Nanoparticles with PARACEST MRI. Molecular Pharmaceutics, 2009, 6, 1409-1416.	4.6	69
90	Using Two Chemical Exchange Saturation Transfer Magnetic Resonance Imaging Contrast Agents for Molecular Imaging Studies. Accounts of Chemical Research, 2009, 42, 915-924.	15.6	103

MARK D PAGEL

18

#	Article	IF	CITATIONS
91	Monitoring infection and inflammation in murine models of cystic fibrosis with magnetic resonance imaging. Journal of Magnetic Resonance Imaging, 2008, 28, 527-532.	3.4	17
92	Languages Evolve in Punctuational Bursts. Science, 2008, 319, 588-588.	12.6	169
93	An overview of responsive MRI contrast agents for molecular imaging. Frontiers in Bioscience - Landmark, 2008, 13, 1733.	3.0	130
94	Peptidyl Molecular Imaging Contrast Agents Using a New Solid-Phase Peptide Synthesis Approach. Bioconjugate Chemistry, 2007, 18, 903-911.	3.6	19
95	Enzymeâ€responsive PARACEST MRI contrast agents: a new biomedical imaging approach for studies of the proteasome. Contrast Media and Molecular Imaging, 2007, 2, 189-198.	0.8	77
96	Design and characterization of a new irreversible responsive PARACEST MRI contrast agent that detects nitric oxide. Magnetic Resonance in Medicine, 2007, 58, 1249-1256.	3.0	112
97	Frequency of word-use predicts rates of lexical evolution throughout Indo-European history. Nature, 2007, 449, 717-720.	27.8	421
98	Bayesian Analysis of Correlated Evolution of Discrete Characters by Reversibleâ€Jump Markov Chain Monte Carlo. American Naturalist, 2006, 167, 808-825.	2.1	809
99	A facile synthesis of α-amino-DOTA as a versatile molecular imaging probe. Tetrahedron Letters, 2006, 47, 7327-7330.	1.4	14

100 The History, Rate and Pattern of World Linguistic Evolution. , 2000, , 391-416.